Journal of Hazardous Materials 209–210 (2012) 34–39

Contents lists available at SciVerse ScienceDirect

Journal of Hazardous Materials

journal homepage: www.elsevier.com/locate/jhazmat

The influence of titanate nanotube on the improved thermal properties and the smoke suppression in poly(methyl methacrylate)

Yangyang Dong[a,b], Zhou Gui[a,*], Yuan Hu[a,**], Yu Wu[a], Saihua Jiang[a]

[a] State Key Laboratory of Fire Science, University of Science and Technology of China, Hefei, 230027, PR China
[b] Department of Chemistry, University of Science and Technology of China, Hefei, 230026, PR China

ARTICLE INFO

Article history:
Received 7 July 2011
Received in revised form
18 November 2011
Accepted 19 December 2011
Available online 16 January 2012

Keywords:
Titanate nanotube
Composite
Thermal property
Smoke suppression
Poly(methyl methacrylate)

ABSTRACT

The well-dispersed poly(methyl methacrylate)/titanate nanotube (PMMA/TNT) composites were synthesized by in situ polymerization of methyl methacrylate (MMA) in ethanol solution. Thermal stability and the glass transition temperature of the composites are significantly enhanced with a proper amount of TNTs. The comparison between PMMA/TNTs and PMMA/TiO_2 composites suggests the formation of network in PMMA/TNTs composite. The coaction of dehydration and the network is believed to be the crucial factor which improves the thermal properties. TG-FTIR analysis shows that the amount of organic volatiles of PMMA is significantly reduced and the non-flammable CO_2 is generated after incorporating TNTs. It implies the reduced toxicity of the volatiles. The possible mechanism of the smoke suppression is proposed as the dehydration and adsorption effect of TNTs.

1. Introduction

Poly(methyl methacrylate) (PMMA) is widely used in industry and medical science, such as building construction, molding and bone cement, but the application is restricted by the associated fire hazards which are caused by the poor thermal stability and the toxic gases generated during combustion. The toxic smoke harm even outpaces the fire itself. Most of the deaths are caused by the toxicity of the smoke. A large amount of toxic fumes is released in the PMMA pyrolysis process, which is composed by small carbon particles and other combustible volatiles, and the flammable methyl methacrylate (MMA) generated in the pyrolysis process further accelerates the decomposition of PMMA [1]. Therefore, it is important to improve the thermal stability and the smoke suppression of PMMA simultaneously. Recently, the novel flame retardants and smoke suppressants are becoming to be halogen-free and non-toxic as the consciousness of environmental protection and safety concern.

Inorganic nanoparticles have been proven to be good additives of PMMA to improve thermal properties of PMMA. Small fraction of the fillers can lead to the significant enhancement of the thermal properties of the polymer [2]. They include layered compounds [3], phosphates [4], and multi-walled carbon nanotubes (MWCNTs) [5], etc. Besides, the inorganic nanoparticles have been widely used as the smoke suppressants to the polymers, such as the metal hydroxides [6,7].

Since the development of hydrothermal synthesis with a high yield by Kasuga et al. [8], titanate nanotubes (TNTs) with a highly specific surface area and ion-exchangeable and photocatalytic abilities have attracted growing interest for wide applications [9,10]. Similar with CNTs, TNTs possess numerous hydroxyl groups [11], which can improve the dispersion in PMMA matrix. Furthermore, the excellent adsorption effect [12] of nanotubes is promising barrier of smoke.

In this work, TNTs were incorporated into PMMA matrix by in situ polymerization. The thermal stability and the glass transition temperature of the PMMA/TNT composites were investigated. The effects of TNTs on the smoke suppression of the PMMA pyrolysis process were discussed. The mechanism of the enhanced thermal stability of the composites and the smoke suppression was proposed. It is looked forward to provide more environment-friendly smoke suppressant, which can enhance the thermal properties simultaneously for the polymers.

2. Experimental

All starting materials used in this work were of analytical grade and were purchased from Sinopharm Chemical Reagent Co., Ltd. MMA was used after further purification, including retarder

* Corresponding author. Tel.: +86 551 3601288; fax: +86 551 3601669.
** Co-corresponding author. Tel.: +86 551 3601664; fax: +86 551 3601664.
E-mail addresses: zgui@ustc.edu.cn (Z. Gui), yuanhu@ustc.edu.cn (Y. Hu).

0304-3894/$ – see front matter © 2011 Elsevier B.V. All rights reserved.
doi:10.1016/j.jhazmat.2011.12.048

removal, water removal and reduced pressure distillation. The other starting materials were used directly.

2.1. Preparation of TNTs

1.5 g of anatase TiO_2 powder was added into 50 mL of 10 M aqueous NaOH solution and the obtained suspension was hydrothermally treated in a sealed Teflon autoclave at 160 °C for 5 h. The resulting precipitate was ground and dispersed in deionized water. The obtained suspension was treated with a 0.1 M HCl solution until pH value reached 2.5 and then stirred for 2 h. The filtrated white precipitate was repeatedly washed with distilled water until the pH value reached 6–7, and the product was dried at 60 °C for 48 h.

2.2. Preparation of PMMA/TNTs and PMMA/TiO_2 composites

Anatase TiO_2 nanoparticles and the synthesized TNTs were dispersed in 10 mL ethanol and mixed with MMA monomer under ultrasound. 0.1 wt% of benzoyl peroxide was added in, and the mixture was stirred at 80 °C for 2 h. The viscous paste was transferred into a mold and held at 70 °C for 48 h in order to complete the polymerization and remove the residual solvent and the unconverted MMA monomer [13].

2.3. Characterization

The X-ray diffraction (XRD) measurement was performed on a Japan Rigaku D/Max-γA X-ray diffractometer with graphite-monochromated Cu Kα radiation (λ = 1.54178 Å). Transmission electron microscopy (TEM) images were obtained on a JEOL JEM-2100F transmission electron microscope at an accelerating voltage of 200 keV. Scanning electron microscopy (SEM) image was recorded on a FEI Co. Ltd. Sirion200 scanning electron microscope at 5 keV acceleration voltage. The thermogravimetric analysis (TGA) was carried out using a SHIMADZU TGA-50 thermoanalyzer instrument under an air flow of 25 mL/min. In each case, the samples (about 5 mg) were heated from room temperature (30 °C) to 700 °C at a linear heating rate of 10 °C/min. Differential scanning calorimetry (DSC) measurements were performed using a PerkinElmer DSC-7 calorimeter under nitrogen flow, samples (about 5 mg) were heated from room temperature (30 °C) to 200 °C and kept for 5 min, then cooled to 30 °C (heating and cooling rate: 20 °C/min). The thermogravimetric analysis/infrared spectrometry (TG-IR) was performed using the TGA Q5000 IR thermogravimetric analyzer which was coupled with the Nicolet 6700 FT-IR spectrophotometer via the transfer line. Each sample specimen (about 5 mg) was carried out at a heating rate of 20 °C/min from room temperature to 700 °C under a nitrogen flow at a flow rate of 35.0 mL/min.

3. Results and discussion

XRD pattern of the synthesized TNTs is shown in Fig. 1. It matches well with standard diffractogram of $H_2Ti_2O_5{\cdot}H_2O$ (JCPDS: 47-0124), which coincides with the general molecular formula of protonated titanate ($H_2Ti_nO_{2n+1}{\cdot}xH_2O$) [14]. From the TEM image (Fig. 2a and b), titanate crystals have typical morphology of nanotube with crystal size of 10 nm in outer diameter, 4 nm in inner diameter and 150 nm in length, and no layered anatase TiO_2 precursor can be observed in the view field. Results above indicate that the anatase TiO_2 has converted to titanate with nanotube morphology entirely.

In order to investigate the inner structure of the composites, composites with the TNT loading of 1.0 wt% and TiO_2 loading of 2.5 wt% were cryogenically broken after immersion in liquid nitrogen and the fractured surface was characterized by SEM. Fig. 3a and b shows that TNTs have good interfacial adhesion with PMMA matrix in the composite, which exhibits uniformly dispersed morphology. From Fig. 3c and d, it can be seen that both the dispersion and interfacial adhesion of anatase TiO_2 nanoparticles are not as well as TNTs in PMMA matrix. It demonstrates that the nanotubes can be better dispersed than TiO_2 nanoparticles in PMMA matrix with in situ polymerization.

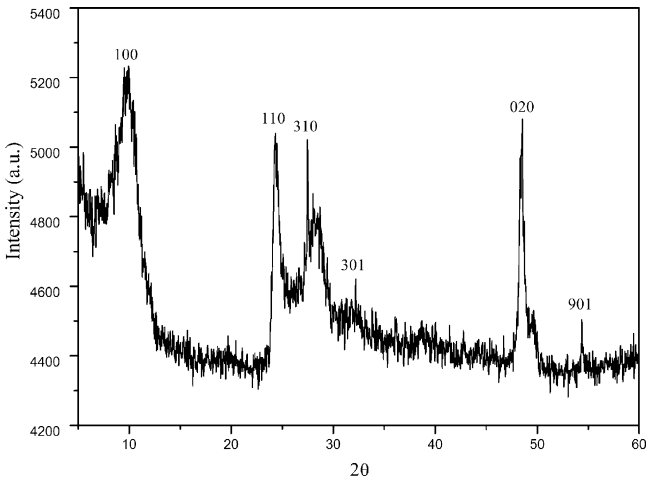

Fig. 1. XRD pattern of the synthesized TNTs.

TGA is one of the most widely used techniques for rapid evaluation of the thermal stability for various polymers. [15] The TGA thermograms of TNTs, pure PMMA and the composites with different loadings in air flows are shown in Fig. 4a. The temperatures at which 10% ($T_{0.1}$) and 50% weight loss ($T_{0.5}$) occur are used as the measures of the onset and half degradation temperature, respectively. The corresponding results are listed in Table 1. In Fig. 4a, pristine TNTs dehydrate at the low temperatures (50–300 °C, weight loss: 11.2 wt%). The TGA curves of the PMMA/TNTs composites have a dramatic shift toward the higher temperature compared with pure PMMA in air flows. In detail, onset and half degradation temperatures of the PMMA/TNTs composites show the same changing tendency. With the increasing loading of TNTs, the two characteristic temperatures of the samples are promoted until the loading of TNTs reach 11.6 wt%. The corresponding $T_{0.1}$ and $T_{0.5}$ of the composite are 298 and 375 °C, which are 54 and 59 °C higher than those of pure PMMA. The characteristic temperatures of the composite with 14.8 wt% TNTs decrease to 291 and 370 °C, which are lower than the sample with 11.6 wt% TNTs. It indicates that the incorporation of proper loading of TNTs enhances the thermal stability of the PMMA composite.

Moreover, it is found that both the $T_{0.1}$ and $T_{0.5}$ of the PMMA/TNTs composites are higher than those of the PMMA/TiO_2 composites, although the loadings of TiO_2 are a bit higher than the corresponding TNTs in the composites (Fig. 4b, Table 1), especially

Table 1
TGA results of TNTs, pure PMMA and the composites with different loadings in air flows.

Composition	$T_{0.1}$ (°C)	$T_{0.5}$ (°C)
PMMA	244	316
PMMA/1.0 wt% TNTs	246	334
PMMA/6.7 wt% TNTs	275	349
PMMA/11.6 wt% TNTs	298	375
PMMA/14.8 wt% TNTs	291	370
PMMA/2.5 wt% TiO_2	230	334
PMMA/12.4 wt% TiO_2	258	341

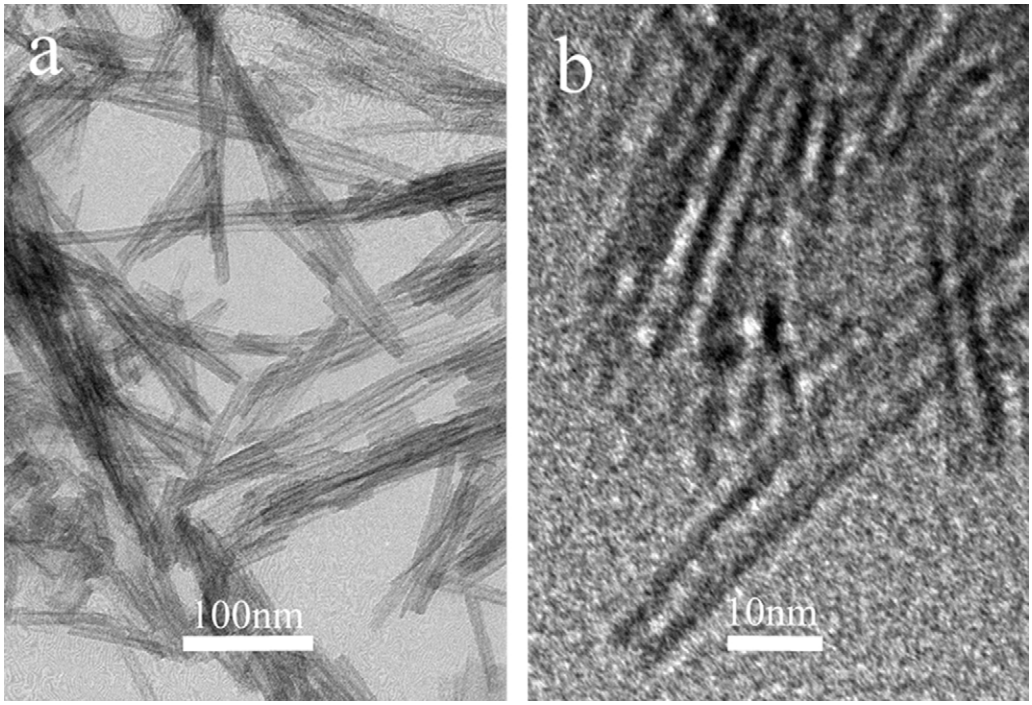

Fig. 2. TEM images of the TNTs at different magnifications.

the onset degradation temperatures. $T_{0.1}$ of the composite with 1.0 wt% and 11.6 wt% TNTs are 2 °C and 54 °C higher than that of pure PMMA, respectively. The corresponding $T_{0.1}$ of 2.5 wt% TiO_2 is 14 °C lower, and 12.4 wt% TiO_2 are 14 °C higher than that of pure PMMA, respectively. It shows that the TNTs can significantly retard the initial thermal degradation compared to TiO_2. It is proposed that the dehydration of TNTs is one of the reasons for the increased onset temperatures, because the heat-absorbing action during evaporation of H_2O leads to the decrease of the heat release. Another possible reason is that the possible network structure in PMMA/TNTs composites enhances the thermal stability.

To verify the existence of the network and its influence in PMMA/TNTs composites, the glass transition temperatures (T_g) of the samples above are tested and calculated by DSC. From Table 2, a significant shift in the T_g of PMMA toward higher temperatures (19 °C) is observed after incorporation of TNTs (1.0 wt% and 6.7 wt%), and the T_g is 10 °C higher than that of the 2.5 wt% PMMA/TiO_2 composite. Further increase of the content of TNTs

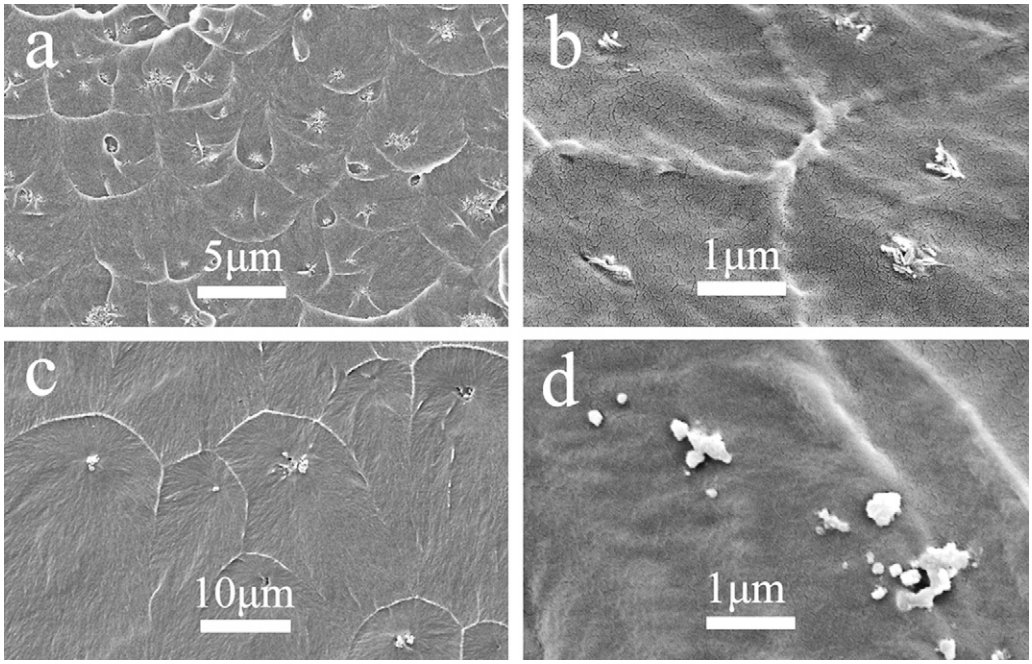

Fig. 3. SEM Images 3a and 3b for the PMMA/TNTs composite (1.0 wt%), 3c and 3d for the PMMA/TNTs composite (2.5 wt%) of the fractured surfaces cryogenically broken after immersion in liquid nitrogen.

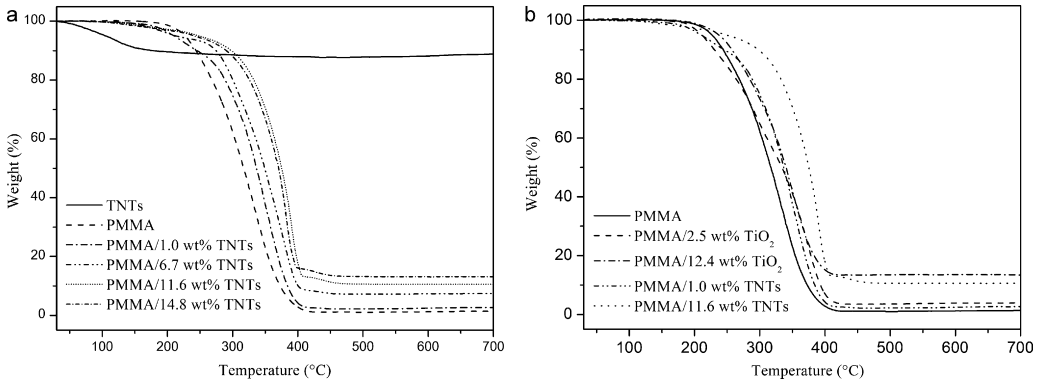

Fig. 4. TGA thermograms of (a) TNTs, pure PMMA and the PMMA/TNTs composites; (b) PMMA and PMMA composites which incorporated TNTs and anatase TiO_2 nanoparticles in air flows.

Table 2
T_g of pure PMMA, PMMA/TNTs and PMMA/TiO_2 composites with different content.

Loading of the filler (wt%)	0	1.0[a]	6.7[a]	11.6[a]	14.8[a]	2.5[b]	12.4[b]
T_g (°C)	104	123	123	107	105	113	119

[a] TNTs.
[b] Anatase TiO_2 nanoparticles.

leads to the decrease of the T_g. However, the increased content of TiO_2 from 2.5 wt% to 12.4 wt% makes T_g of PMMA/TiO_2 composite increase by 6 °C. The difference suggests the network in PMMA/TNTs composites, because the network and good interfacial interaction between nanotubes and the matrix in PMMA/TNTs restrict the molecular mobility of the PMMA chains [16]. The network makes the segmental motion of PMMA in PMMA/TNTs composite more difficult than in PMMA/TiO_2 composite. And then the thermal stability of the PMMA/TNTs composite is enhanced. However, excessive TNTs segment the matrix. The crystallinity of PMMA is reduced, and then the T_g is decreased. It is believed that the decreased crystallinity of PMMA would lead to a lower thermal stability. Therefore, the thermal stability of 14.8 wt% PMMA/TNTs composite is lower than that of 11.6 wt% PMMA/TNTs composite.

TGA and DSC tests above suggest that the thermal stability of the polymer is effectively improved by incorporating the proper amount of TNTs. The comparison of degradation temperature and T_g between PMMA/TNTs and PMMA/TiO_2 composites suggests that the network has formed in the PMMA/TNTs composites. The combined action of the network in PMMA/TNTs composite and dehydration of the nanotubes retards thermal degradation of PMMA significantly.

To investigate the influence of TNTs on the evolved gaseous volatiles during pyrolysis, the volatile components of PMMA and the composite (14.8 wt% TNTs) are investigated by TG-FTIR technique [17]. The 3D diagrams of PMMA and PMMA/TNTs composite (14.8 wt%) are shown in Fig. 5. It shows that the typical thermal degradation process of the composite is similar to pure PMMA. The absorbance at about 2358 cm^{-1} shows the generation of CO_2 during pyrolysis of the composite, which cannot be found in thermal degradation of pure PMMA.

In order to provide a clear comparison, FTIR spectra of the gaseous volatiles evolved at different temperatures corresponding to the maximum evolve intensity of organic volatiles (PMMA: 485.6 °C, PMMA/TNTs: 328.6 °C) and CO_2 (365.8 °C) are represented in Fig. 6. It can be seen that most of the characteristic peaks of the volatile products of PMMA/TNTs composite are similar to those of PMMA. It indicates that the composition of the gaseous products of the samples is similar. The bands at 3467–3570 cm^{-1} are due to the vibration absorption of hydroxide groups, which indicates the generation of H_2O. The FTIR spectra also show the characteristic bands of hydrocarbons. The aliphatic C—H band at 2965 and 1447 cm^{-1} is produced by n-alkanes. Peaks at 1650 and 937 cm^{-1} indicate the formation of the alkenes. The characteristic peak at 1753 cm^{-1} is due to the absorbance of stretching vibration of C=O band, and peaks at 1307 and 1167 cm^{-1} is caused by the C—O bond. The relative intensity of characteristic peak of carbon dioxide at 2358 cm^{-1} is increased when the temperature increases from 328.6 °C to 365.8 °C. It means that the generation of CO_2 follows the organic volatiles. Therefore, dilution of the flammable gases by the non-flammable CO_2 is possible in the gas phase [18]. Then the thermal degradation is possible to be retarded.

Fig. 7 gives the intensity of typical gaseous organic volatiles of pure PMMA and the PMMA/TNTs composite. The maximum intensity of the evolved products has reduced to 64% of those evolved by pure PMMA, which implies that the amount of the volatiles released

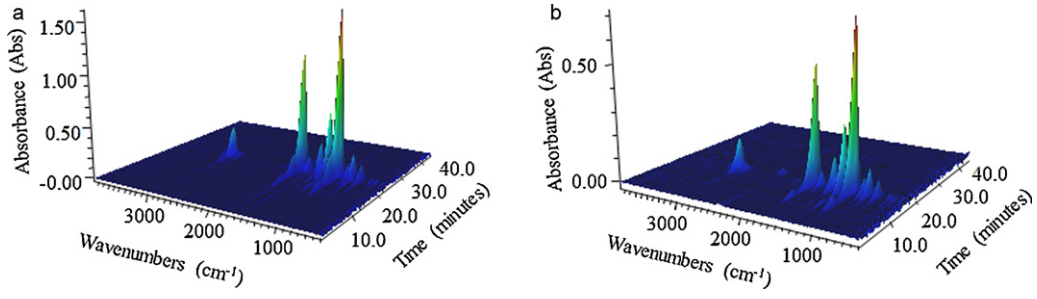

Fig. 5. The 3D diagrams of the gaseous volatiles during combustion process of (a) pure PMMA and (b) PMMA/TNTs composite (14.8 wt%).

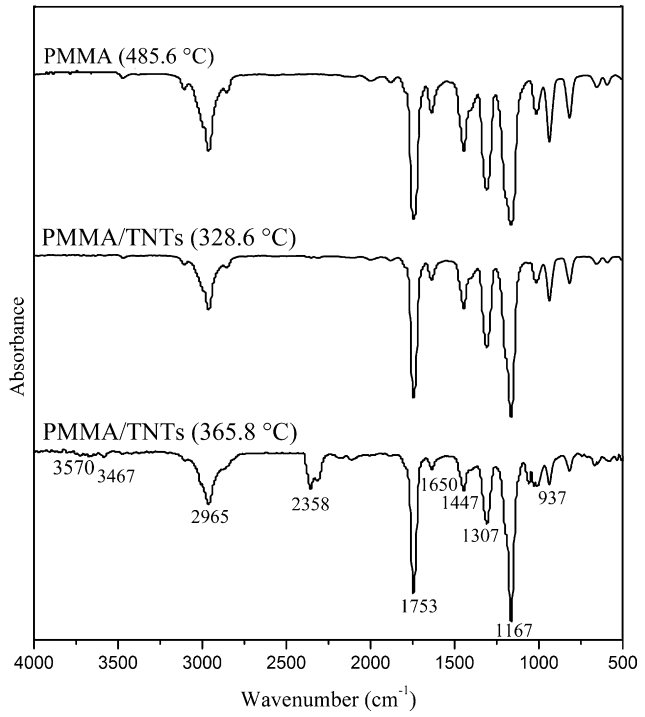

Fig. 6. IR spectra of gasified pyrolysis products for pure PMMA at 485.6 °C and PMMA/TNTs composite (14.8 wt%) at 328.6 and 365.8 °C.

from the PMMA/TNTs composite is much less than that from the pure PMMA [19]. The reduced amount of the organic volatiles further leads to the inhibition of smoke, because the organic volatiles may crack into smaller hydrocarbon molecules and smoke particles. The gaseous hydrocarbons are condensed and the smoke particles are aggregated to form smoke.

The adsorption effect of TNTs is proposed to be the possible reason for the generation of CO_2 and the reduction of organic volatiles. The PMMA decomposes via the free radical chain depolymerization. TNTs have large specific surface area, and they are apt to absorb the small gaseous molecules [13]. Here the TNTs may absorb the free radicals and MMA molecules which are generated during the depolymerization of PMMA. It partly terminates the chain depolymerization and retards the escape of the organic volatiles. The free radicals and MMA molecules then further evolve into the non-flammable CO_2. In addition, the dehydration of TNTs is helpful

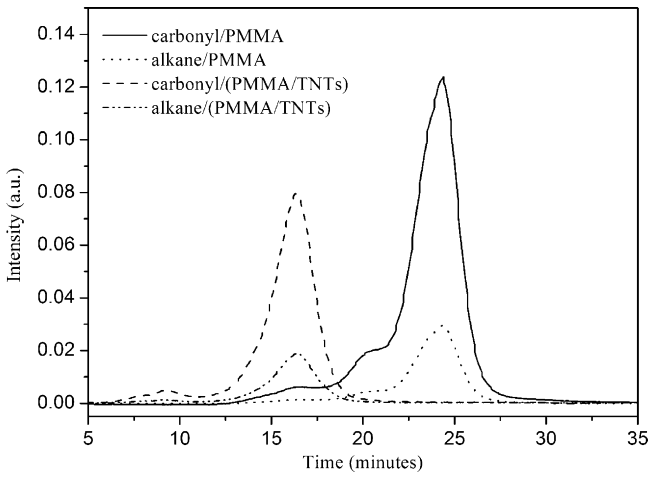

Fig. 7. Intensity of characteristic peaks for pyrolysis products of PMMA and the PMMA/TNTs composite (14.8 wt%).

to reduce the toxicity of the volatiles. The water vapor dilutes or absorbs hydrocarbon particles, and produces H_2 and CO at the high temperatures. These H_2 and CO are burnt out into CO_2 and H_2O, thereby the toxicity of combustion products is reduced [20].

In summary, the possible mechanisms of the improved thermal properties of PMMA and the reduced combustion products are proposed as follows: first, the network structure of the PMMA/TNTs composite plays a key role in improving the thermal properties. The network constructed by one-dimensional TNTs can effectively induce the mobility restriction of polymer chains, thus retards the thermal degradation of PMMA. Second, the absorption effect of TNTs decreases the amount of organic volatiles. The generated non-flammable CO_2 is conducive to retard the pyrolysis of PMMA. Third, the dehydration of hydroxyl groups on nanotubes at the initial thermal degradation reduces the heat flow and promotes the onset degradation temperatures of the composites. The water vapor also reduces the toxicity of the volatiles by reacting with hydrocarbon particles.

4. Conclusion

The well-dispersed PMMA/TNTs composites were synthesized by in situ polymerization of MMA. TGA test shows that the thermal stability of PMMA is significantly enhanced by incorporating the proper amount of TNTs. The comparison between PMMA/TNTs and PMMA/TiO_2 composites indicates that the initial degradation of PMMA is retarded. TNTs with low content enhance T_g of the polymer greatly, and with higher content, the T_g decreases. It is proposed that network has formed in the PMMA/TNTs. The network structure is believed to be an important factor to the enhanced thermal stability and T_g. The dehydration of TNTs is considered to be helpful to retard the initial thermal degradation. In addition, because of the effects of absorption and dehydration of TNTs, the amount of the harmful organic volatiles is reduced, and the non-flammable CO_2 is generated. We believe that the investigation will stimulate further efforts in improving thermal properties and suppressing smoke in combustion for polymers.

Acknowledgments

This work was supported by the National Natural Science Foundation of China (No. 21071138) and National Basic Research Program of China (973 Program) (No. 2012CB922002).

References

[1] H.S. Taylor, A.V. Tobolsky, Radical chain processes in vinyl and diene reactions, J. Am. Chem. Soc. 67 (1945) 2063–2067.
[2] E.J. García, A.J. Hart, B.L. Wardle, A.H. Slocum, Fabrication and nanocompression testing of aligned carbon-nanotube-polymer nanocomposites, Adv. Mater. 19 (2007) 2151–2156.
[3] C. Manzi-Nshuti, D.Y. Wang, J.M. Hossenlopp, C.A. Wilkie, Aluminum-containing layered double hydroxides: the thermal, mechanical, and fire properties of (nano)composites of poly(methyl methacrylate), J. Mater. Chem. 18 (2008) 3091–3102.
[4] D.D. Yang, Y. Hu, L. Song, S.B. Nie, S.Q. He, Y.B. Cai, Catalyzing carbonization function of α-ZrP based intumescent fire retardant polypropylene nanocomposites, Polym. Degrad. Stab. 93 (2008) 2014–2018.
[5] T. Kashiwagi, F.M. Du, J.F. Douglas, K.I. Winey, R.H. Harris, J.R. Shields, Nanoparticle networks reduce the flammability of polymer nanocomposites, Nat. Mater. 4 (2005) 928–933.
[6] T. Xu, X. Huang, A TG-FTIR investigation into smoke suppression mechanism of magnesium hydroxide in asphalt combustion process, J. Anal. Appl. Pyrolysis 87 (2010) 217–223.
[7] H.M. Zhu, X.G. Jiang, J.H. Yan, Y. Chi, K.F. Cen, TG-FTIR analysis of PVC thermal degradation and HCl removal, J. Anal. Appl. Pyrolysis 82 (2008) 1–9.
[8] T. Kasuga, M. Hiramatsu, A. Hoson, T. Sekino, K. Niihara, Titania nanotubes prepared by chemical processing, Adv. Mater. 11 (1999) 1307–1311.
[9] Y.K. Zhou, L. Cao, F.B. Zhang, B.L. He, H.L. Li, Lithium insertion into TiO_2 nanotube prepared by the hydrothermal process, J. Electrochem. Soc. 150 (2003) A1246–A1249.

[10] Y. Ohsaki, N. Masaki, T. Kitamura, Y. Wada, T. Okamoto, T. Sekino, K. Niihara, S. Yanagida, Dye-sensitized TiO_2 nanotube solar cells: fabrication and electronic characterization, Phys. Chem. Chem. Phys. 7 (2005) 4157–4163.
[11] T. Kasuga, Formation of titanium oxide nanotubes using chemical treatments and their characteristic properties, Thin Solid Films 496 (2006) 141–145.
[12] S. Funk, B. Hokkanen, U. Burghaus, A. Ghicov, P. Schmuki, Unexpected adsorption of oxygen on TiO_2 nanotube arrays: influence of crystal structure, Nano Lett. 7 (2007) 1091–1094.
[13] M. Avella, M.E. Errico, E. Martuscelli, Novel PMMA/$CaCO_3$ nanocomposites abrasion resistant prepared by an in situ polymerization process, Nano Lett. 1 (2001) 213–217.
[14] A.R. Armstrong, G. Armstrong, J. Canales, TiO_2-B nanowires, Angew. Chem. Int. Ed. 43 (2004) 2286–2288.
[15] X. Cheng, S.Y. Liu, W.F. Shi, Synthesis and properties of silsesquioxane-based hybrid urethane acrylate applied to UV-curable flame-retardant coatings, Prog. Org. Coat. 65 (2009) 1–9.
[16] M. Inkyo, Y. Tokunaga, T. Tahara, T. Iwaki, F. Iskandar, C.J. Hogan Jr., K. Okuyama, Beads mill-assisted synthesis of poly methyl methacrylate (PMMA)–TiO_2 nanoparticle composites, Ind. Eng. Chem. Res. 47 (2008) 2597–2604.
[17] W.Y. Xing, L. Song, Y. Hu, S. Zhou, K. Wu, L.J. Chen, Thermal properties and combustion behaviors of a novel UV-curable flame retarded coating containing silicon and phosphorus, Polym. Degrad. Stab. 94 (2009) 1503–1508.
[18] T. Rajkumar, C.T. Vijayakumar, P. Sivasamy, B. Sreedhar, C.A. Wilkie, Thermal degradation studies on PMMA–HET acid based oligoesters blends, J. Therm. Anal. Calorim. 100 (2010) 651–660.
[19] K. Wu, Y. Hu, L. Song, H.D Lu, Z.Z. Wang, Flame retardancy and thermal degradation of intumescent flame retardant starch-based biodegradable composites, Ind. Eng. Chem. Res. 48 (2009) 3150–3157.
[20] X.L. Chen, J. Yu, S.Y. Guo, Structure and properties of polypropylene composites filled with magnesium hydroxide, J. Appl. Polym. Sci. 102 (2006) 4943–4951.